J. Mater. Environ. Sci. 6 (12) (2015) 3496-3500
ISSN : 2028-2508
CODEN: JMESCN

CO_2 sensing characteristics of CuO/Spinel thin films deposited on micro-heater

F. Oudrhiri-Hassani[1*], L. Presmanes[2], A. Barnabe[2], A. Kammouni[3], P. Tailhades[2]

[1] *LMPEQ, Université Cadi Ayyad, ENSA de Safi, Route Sidi Bouzid BP 63, 46000 Safi, Maroc.*
[2] *Institut Carnot Cirimat ; 118 Route de Narbonne 31062 Toulouse cedex 09, France.*
[3]*Ecole Nationale Supérieure d'Arts et Métiers de Casablanca, Hassan II University of Casablanca, Casablanca, Maroc.*

[*]*Corresponding Author. E-mail: fahd_oudrhiri@yahoo.fr; Tel: (+212677023915)*

Abstract
Gas sensing films are prepared by radiofrequency sputtering method. These films are made of p-type CuO and n-type $Cu_xFe_{3-x}O_4$ semi-conductors oxides. In order to determine and to improve the CO_2 sensing characteristics, a micro-heater has been used as substrate on which the sensitive layer is deposited. The substrate is then placed into a chamber to operate under controlled atmosphere and to make electrical measurements. Response of thin film to carbon dioxide is analyzed as a function of concentration and at different working temperatures (between 150 and 400 °C). The results show a maximum of sensitivity at 200°C with a good response time.

Keywords: Oxides, Sputtering, Gas sensor, Carbon dioxide, Thin films

Introduction
Global climatic warming is one of the major concerns of this century. According to some researchers, this phenomenon may be related to air pollution and emissions of greenhouse gases such as CO_2. The control of these emissions requires a gas sensor development, especially CO_2 gas sensors. The latter, could be used in many different applications fields such as: habitats, cars, food processing and CO_2 storage sites.
Currently, CO_2 sensors has been using mainly in electrochemical and infrared methods, but these devices are cumbersome, expensive and has a low selectivity in the presence of interfering gases like CO and humidity. Another way is to use metal oxides semiconductor as sensitive materials, which based on the adsorption of a gas and resulted in the variation of electrical conductivity. Indeed, for a n-type semiconductor, the adsorption of an oxide gases which are electron acceptors (such as O_2), trap electrons from the surface of the semiconductor, leading to a decreasee of the resistance. Until now, studies have been carried out exclusively on two families of oxides: CuO-$BaTiO_3$ [1-4] and SnO_2 [5-7]. These materials have often been used as thin films for gas sensor applications, because they have enhanced compatibility with microfabrication techniques and lower power consumption. In this paper we have investigated the CO_2 sensing characteristics of nanocomposites thin films elaborated by radio-frequency sputtering. These films are made of copper oxide CuO and spinel phase $Cu_xFe_{3-x}O_4$.

2. Experimental Methods
2.1. Films preparation
The thin films are deposited with an Alcatel A450 apparatus using a sintered ceramic target of pure $CuFeO_2$ with a relative density of 70%. The RF power is fixed at $4W/cm^2$ and the pressure inside the deposition chamber is 5×10^{-6} mbar. During the deposition of the films, the argon pressure and the target-to-substrate distance are kept at 0.5 Pa and 5 cm respectively. Thin films of 300 nm are deposited on glass substrate for structural characterizations. The film thickness is fixed to a value of 50 nm when making the sensor device for CO_2 sensing tests.
Thickness measurements are performed with a DEKTAK 3030ST profilometer. The structural properties are determined by grazing angle X-ray diffraction (α=1) with a Siemens D5000 diffractometer (Cu Kα:

λ=0.15418nm). The microstructure of thin films is characterized by JEOL 2100 Transmission Electron Microscope (TEM) operating at 200 kV equipped with a X-ray Energy Dispersive Spectroscopy (X-EDS) system.

2.2. Sensor fabrication

In this work, $Cu_xFe_{3-x}O_4$- CuO nanocomposites thin films have been tested for carbon dioxide monitoring. Our test device (Figure 1) integrates a temperature sensor (Pt1000), a heater and interdigitated electrode structures (IDES) in platinum thin film on a ceramic substrate. Heater and sensor are covered with an insulating glass layer. The heat resistance is connected to an AC voltage generator. The chip can be kept at a constant temperature or a temperature cycle can be operated. As shown in figure (1.b), the sensing nanocomposite layer is then deposited over top of the platinum electrodes by the sputtering method mentioned above. The electrical response of the sensing layer is investigated by registering the variations in impedance with a RCL-meter (FLUKE PM6306) as a function of temperature, time and gas concentration. The test device is placed into a small chamber operating under controlled atmosphere with the temperature range of 20–450 °C. The tests are performed under a fixed flux of 50 sccm. A low frequency of 700 Hz is used to avoid the relaxation phenomena[8]. The response R is determined by the following equation:

$$R= 100\times((Z_{CO2} - Z_{air}) / Z_{air}) \qquad \text{(Eq. 1)}$$

where Z_{air} and Z_{CO2} are the electrical impedances of the sensor measured in air and in CO_2 respectively.

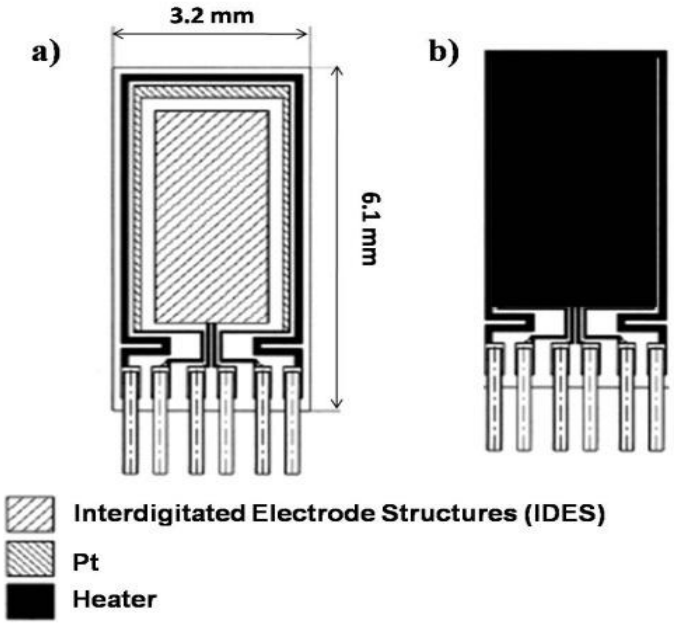

Figure 1: Schematic of test device (a) before deposition (b) after deposition of nanocomposite sensing layer.

3. Results and discussion

3.1 Structural characterization

The elaboration process of sensitive layer begins with the deposition of the film by rf-sputtering. In the Figure(2.a), the GXRD pattern of the as-deposited thin film shows clearly the presence of two peaks at 2θ = 43.3° and 2θ = 50.43° which corresponds to metal copper. The broad peak located at 2θ = 35.5° can be attributed to the various mixed oxide phases, such as CuO, $CuFeO_2$ and/or $CuFe_2O_4$. TEM image of as-deposited sample of 50nm thickness (Figure 3) shows grains of nanometric size from 20 to 25 nm and a of the larger clusters dispersed on surface. We note also the existence of zones from which contrasts are different. The dark zones correspond to metal copper clusters.

The studied samples are thus composed primarily of two phases: metal copper and oxide phases. The rf-sputteirng of $CuFeO_2$ target leads to the formation of reduced species in the film. This reduction is favoured by the low oxygen pressure during the deposition and the bombardment of the target and the substrate by various energetic species (cations, secondary electrons, retro-diffused argon).

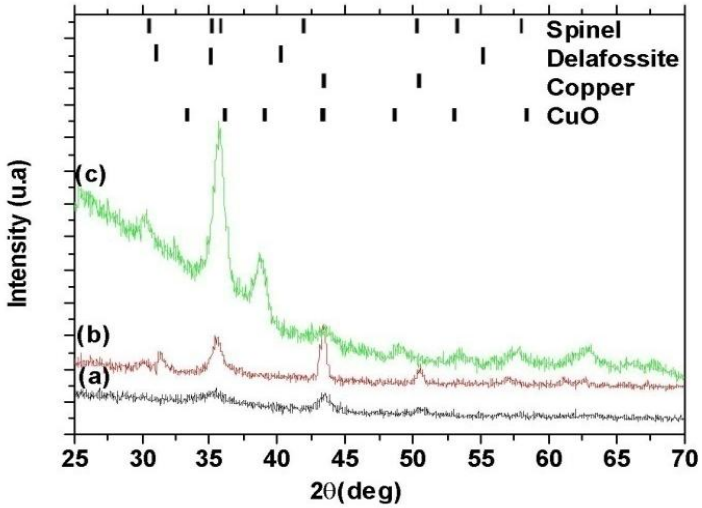

Figure 2: Grazing angle X-ray diffraction (GXRD) patterns of the deposited film on glass substrate from a $CuFeO_2$ target, (a) as-deposited film, (b) after annealing film under vacuum at 450 °C and (c) after annealing in air at 450 °C. Thickness of film = 300 nm.

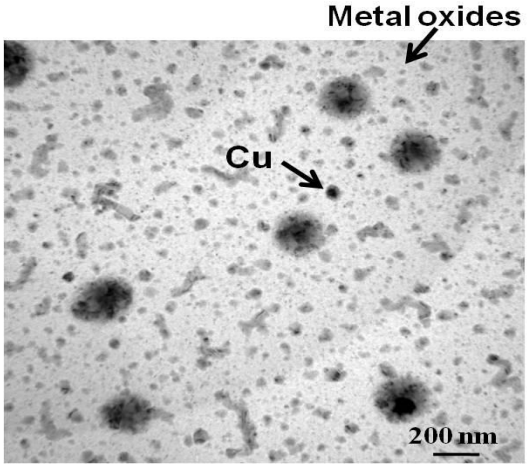

Figure 3: TEM image of as-deposited sample of 50 nm thickness.

The reduction of the target $CuFeO_2$ at the time of the deposit can then be represented by the following equation [9]:

$$CuFeO_2 \rightarrow (\frac{1}{3-x})Cu_xFe_{3-x}O_4 + (\frac{3-2x}{3-x})Cu + (\frac{1-x}{3-x})O_2 \qquad \text{(Eq. 2)}$$

However, sputtering deposition is an out-of-equilibrium process and during the thin film deposition, the equation (2) is not complete. In addition to spinel and metallic copper, the nanocrystalline delafossite phase is also present in the final deposited compound [10], but it cannot be identified by using GXRD due to the nanocrystallinity of deposited phases. An additional thermal annealing under vacuum at 450°C is performed in order to increase the crystallite size of the phases (Figure 2.b). Two peaks of delafossite are observed at 2θ=31.2° and 2θ = 35.7°. This last however, is partially superimposed on that of the spinel phase.

The next step in elaboration of CuO-$Cu_xFe_{3-x}O_4$ consists in carrying out a heat treatment of as-deposited thin films in air at 450°C (Figure 2.c). The two principal peaks of the tenorite (CuO) phase appear at 2θ = 35.5° and 2θ = 38.7°. The presence of CuO is due mainly to the oxidation of metal copper initially present in as-prepared sample. On the other hand, it has already been demonstrated that the $CuFeO_2$ phase can be dissociated in air into $CuFe_2O_4$ and CuO phases [10].

In conclusion, RF-sputtering method allows us to obtain a homogeneous and nanosized composite thin films constituted of two semiconductor materials p-type CuO and n-type $Cu_xFe_{3-x}O_4$.

3.2. CO_2 sensing characteristics

Typical static and transient characteristics of the sensor to carbon dioxide are shown in Figure 4. The electrical impedance of the nanocomposite layer is decreased by injection of CO_2 gas, which implies a negative response ($R<0$) because $Z_{CO2}<Z_{air}$. This variation let us assume that the oxidizing gas such us CO_2 (electron acceptor) interacts with a p-type semi-conductor by increasing the number of holes. Thus, it appears that the interactions of CO_2 with the copper oxide (CuO) contribute significantly to variations in electrical properties of nanocomposites. We have seen in previous paper [11] that the interaction of CuO-$Cu_xFe_{3-x}O_4$ with a reducing gas such as CO lead to a positive response and then also react like in the presence of a *p*-type semiconductor. We can also observe that the signal is reversible and the stabilization under CO_2 gas don't take long time compared to the tests carried out on CuO-$Cu_xFe_{3-x}O_4$ thin films deposited on gold interdigitated electrodes [12]. The response and recovery times are both 25 minutes and 10 minutes respectively. It is interesting to note that the microstructure play an important role in the gas sensing properties of the films. The rf-sputtering allows us to prepare a microporous films with small grains size [13]. These parameters influence positively the response of the films [14, 15].

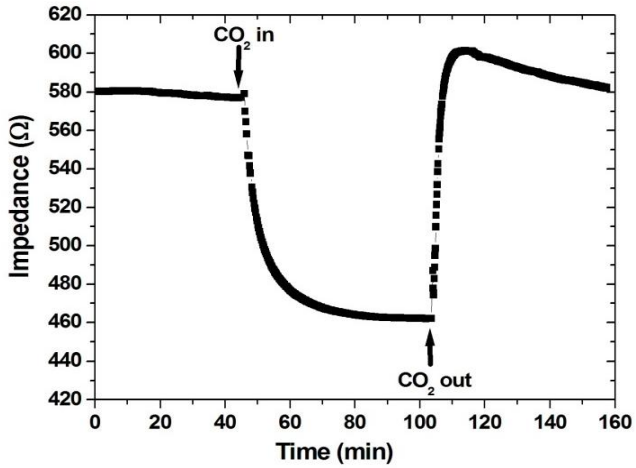

Figure 4: Impedance transient for response and recovery of CuO-$Cu_xFe_{3-x}O_4$ sensing layer. f = 700 Hz, T=200 °C, flow = 50 sccm, [CO_2] = 5000 ppm, Thickness = 50 nm.

In order to find out the optimum operating temperature, many CO_2 gas sensing experiments have been performed at different temperatures. Figure 5 shows the variation of response magnitude as a function of temperature.

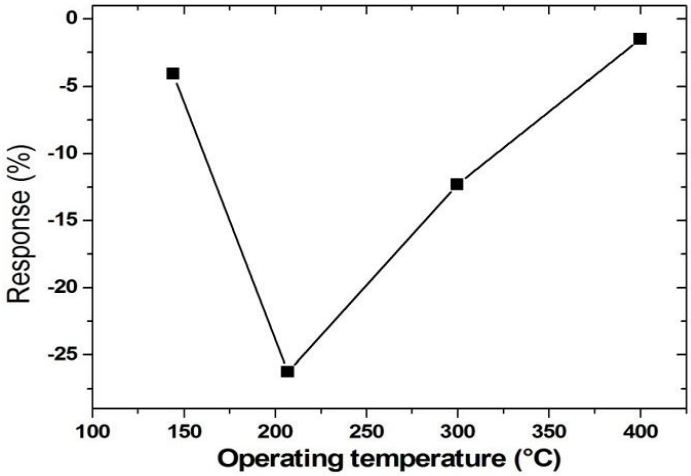

Figure 5: Response as a function of operating temperature of the CuO-$Cu_xFe_{3-x}O_4$ layer deposited on micro-heater. f = 700 Hz, flow = 50 sccm, [CO_2] = 5000 ppm, Thickness = 50 nm.

A maximum response around -27 % is obtained at 200 °C which corresponds to a Z_{CO2}/Z_{air} ratio of 0.8. This response is mainly due to the adsorption of molecules on the surface of the films. Below 200 °C, the presence of hydroxyl groups and carbonate may lead to inhibition of sensor performance. At 200 °C, the desorption of

contaminants make more sites available for the adsorption of sensory species. At higher temperature, the decrease of the response results from the surface desorption of the sensory species which are responsible for changing the response factor.

To monitor the response of the active layer as a function of CO_2 concentration, we vary the CO_2 content in the air at the optimum temperature of 200 °C (Figure 6). An increase of CO_2 concentration leads to the increase of the sensitivity of the layer; this means that the number of molecules which react with the adsorption sites increases.

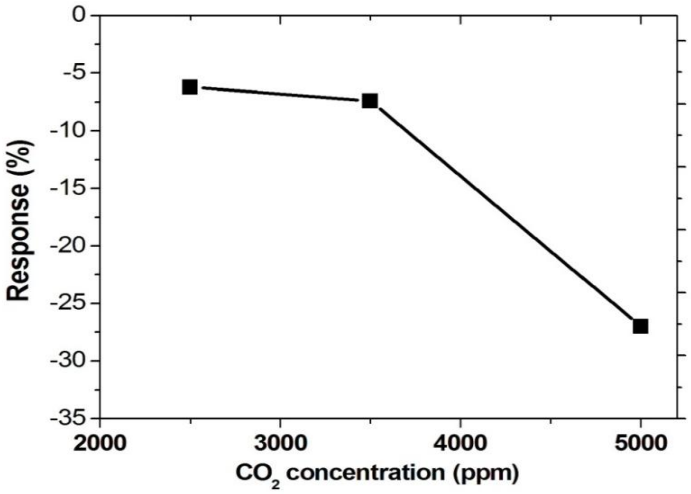

Figure 6: Response of CuO-$Cu_xFe_{3-x}O_4$ layer as a function of CO_2 concentration. f = 700 Hz, T = 200 ◦C, thickness = 50 nm.

Conclusion

This study presents the CO_2 sensing properties of CuO/$Cu_xFe_{3-x}O_4$ thin films deposited by radio-frequency sputtering method. The use of a mico-heater platform with IDES platinum electrodes leads to obtain a maximum response of -27% to 5000 ppm at low temperature of 200°C. Furthermore, for a sensor to be useful, the characteristics can be improved vastly by means of doping and catalyzing with different elements.

References

1. Herran J., Mandayo G.G., Ayerdi I., Castano E., *Sens. Actuators B* 129 (2008) 386.
2. Liao B., Wei Q., Wang K., Liu Y., *Sens. Actuators B* 80 (2001) 208.
3. Ishihara T., Kometani K., Nishi Y., Takita Y., *Sens. Actuators B* 28 (1995) 49.
4. Haeusler A., Meyer J.U., *Sens. Actuators B* 34 (1996) 388.
5. Steiner K., Hoefer U., Kühner G., Sulz G., Wagner E., *Sens. Actuators B* 25 (1995) 529.
6. Dong Hyun Kim, Ji Young Yoon, Hee Chan Park, Kwang Ho Kim, *Sens. Actuators B* 62 (2000) 61.
7. Ehsani M., Hamidon M. N., *Int J Appl Electr. Phys. & Robot* 2 (2014) 6.
8. Herrán J., Mandayo G.G., Castano E., *Sens. Actuators B* 127 (2007) 370.
9. Katkov A.E., Lykasov A.A., *Inorg. Mater.* 39 (2003) 171.
10. Mugnier E., Pasquet I., Barnabe A., Presmanes L., Bonningue C., Tailhades P., *Thin Solid Films* 493 (2005) 49.
11. Presmanes L., Chapelle A., Oudrhiri-Hassani F., Barnabe A., and Tailhades P., *Sens. Letters* 9 (2011) 587.
12. Chapelle A., Oudrhiri-Hassani F., Presmanes L., Barnabe A., Tailhades P., *Appl. Surf. Sci.* 256 (2010) 4715.
13. Oudrhiri-Hassani F., Presmanes L., Barnabé A., Tailhades P., *Appl. Surf. Sci.* 254 (2008) 5796.
14. Tamaki J., Zhang Z., Fujimori K., Akiyama M., Harada T., Yamazoe N., *J. Electrochem. Soc.* 141 (1994) 2207.
15. Majumdar S., *Ceramics International* 41(2015)14350.